Electronic Supplementary Material (ESI) for Materials Chemistry Frontiers.

Supporting Information

Regulating the species and the counter-ions size of proton acids to prepare novel poly(4-aminodiphenylamine) nanomaterials towards supercapacitor

Rui Zhao, Hui Peng, Faqiang Wang, Jianghong Zhen, Lu Li, Guofu Ma and Ziqiang Lei**

Key Laboratory of Eco-functional Polymer Materials of the Ministry of Education, Key Laboratory of Polymer Materials of Gansu Province, College of Chemistry and Chemical Engineering, Northwest Normal University, Lanzhou 730070, China.

*Corresponding authors. penghui@nwnu.edu.cn (H. Peng), leizq@nwnu.edu.cn (Z. Lei).

S1. Characterization

Field emission scanning electron microscopy (FE-SEM) images were characterized using a JSM-6701F Japan at an accelerating voltage of 5.0 kV, and transmission electron microscopy (TEM) images were characterized using a JEM-2010 Japan. X-ray diffraction (XRD) patterns were examined on a diffractometer (D/Max-2400, Rigaku) advance instrument with Cu K_α radiation (k =1.5418 Å) at 40 kV, 100 mA with 2θ range from 5 to 80°. Fourier transform infrared (FTIR) transmission spectra were obtained on a DIGILAB FTS-3000 (American Digilab Company). The zeta potential measurements were conducted on a zetasizer nanosystem (Nano ZS, Malvern Instruments) and each solution for zeta potential study was diluted 10,000 times.

S2. Fabrication of three-electrode system

Firstly, the electroactive material was mixed with polyvinylidene fluoride (PVDF) and commercial carbon black with a mass ratio of 80:10:10, followed by adding N-methyl-2-pyrrolidone (NMP) to form homogeneous slurry. Subsequently, the obtained slurry was coated on nickel foam (working area ≈ 1.0 cm^2) and then dried at 60 ℃ for 12 h. Herein, the three-electrode system was test in 1 M H_2SO_4 electrolyte with high purity carbon rod as the counter electrode and saturated calomel electrode (SCE) as the reference electrode. And the mass loadings of each electrode (4-ADPA)-H, P(4-ADPA)-P, P(4-ADPA)-S, P(4-ADPA)-M, P(4-ADPA)-C, P(4-ADPA)-L-0.5 and P(4-ADPA)-L-2 are 3.28, 3.20, 3.36, 3.44, 3.20, 3.28, 3.44 and 3.28 mg, respectively.

S3. Symmetric supercapacitor fabrication

Concretely, the electroactive material with polyvinylidene fluoride (PVDF) and commercial carbon black (8:1:1) was mixed in N-methyl-2-pyrrolidone (NMP) to form a homogeneous slurry. Then, the slurry was coated on carbon sheet with a working area of 1.0 cm^2 and dried at 60 ℃ for 12 h. Finally, two P(4-ADPA) electrodes were pressed together and separated by a thin filter paper and the loading

mass of P(4-ADPA) was 3.04 mg. The electrochemical measurements were carried out in a two-electrode cell at room temperature in 1 M H_2SO_4 electrolyte.

S4. Electrochemical measurements

The electrochemical properties of the samples were investigated by cyclic voltammetry (CV) and galvanostatic charge/discharge measurements in three-electrode cell and two-electrode configuration using a CHI 660D electrochemical workstation. The cycle-life stability was performed using computer controlled cycling equipment (LAND CT2001A, Wuhan China). Electrochemical impedance spectroscopy (EIS) measurements were performed with the Autolab PGSTAT 128N equipped (Eco-chemie, Netherland) with FRA module, the frequency ranging from 10 mHz to 100 kHz and an impedance amplitude of ±5 mV at open circuit potential.

The gravimetric capacitance from galvanostatic charge/discharge was calculated by using the formula of $C_s=4I\Delta t/(m\Delta V)$ for the two-electrode system, while, $C_s^*=I\Delta t/(m\Delta V)$ for the three-electrode system, where I is the constant current (A) and m is the mass (g) of electrode material (For the two-electrode cells, m is the total mass of positive and negative electrodes), Δt the discharge time and ΔV the voltage change during the discharge process.

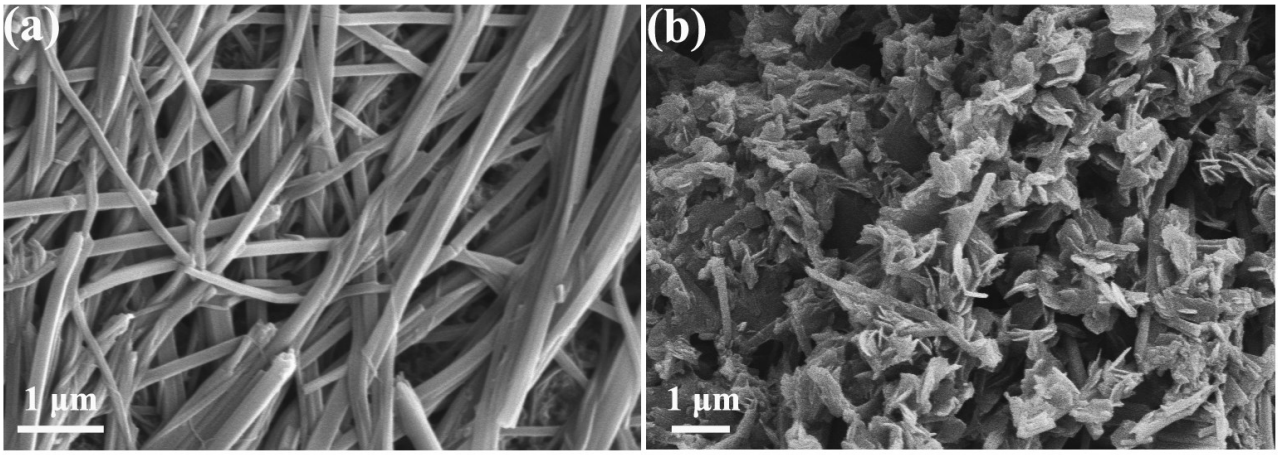

Figure S1 FE-SEM images of (a) P(4-ADPA)-L-0.5 and (b) P(4-ADPA)-L-2.

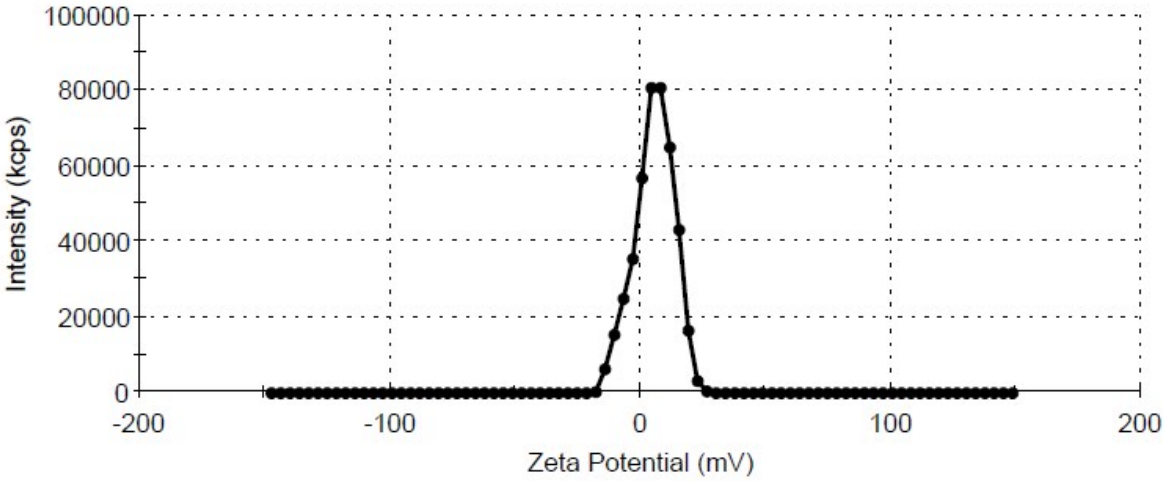

Figure S2 Zeta potential curve of 2 mmol CTAB in deionized water.

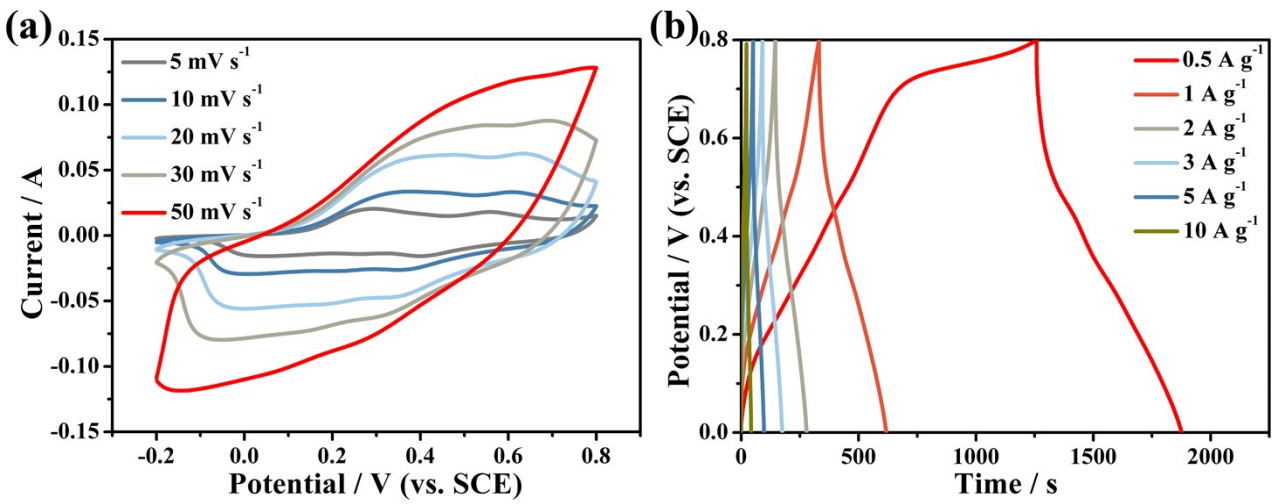

Figure S3 (a) CV curves at different scan rates; (c) the GCD curves at different current densities of P(4-ADPA)-L.

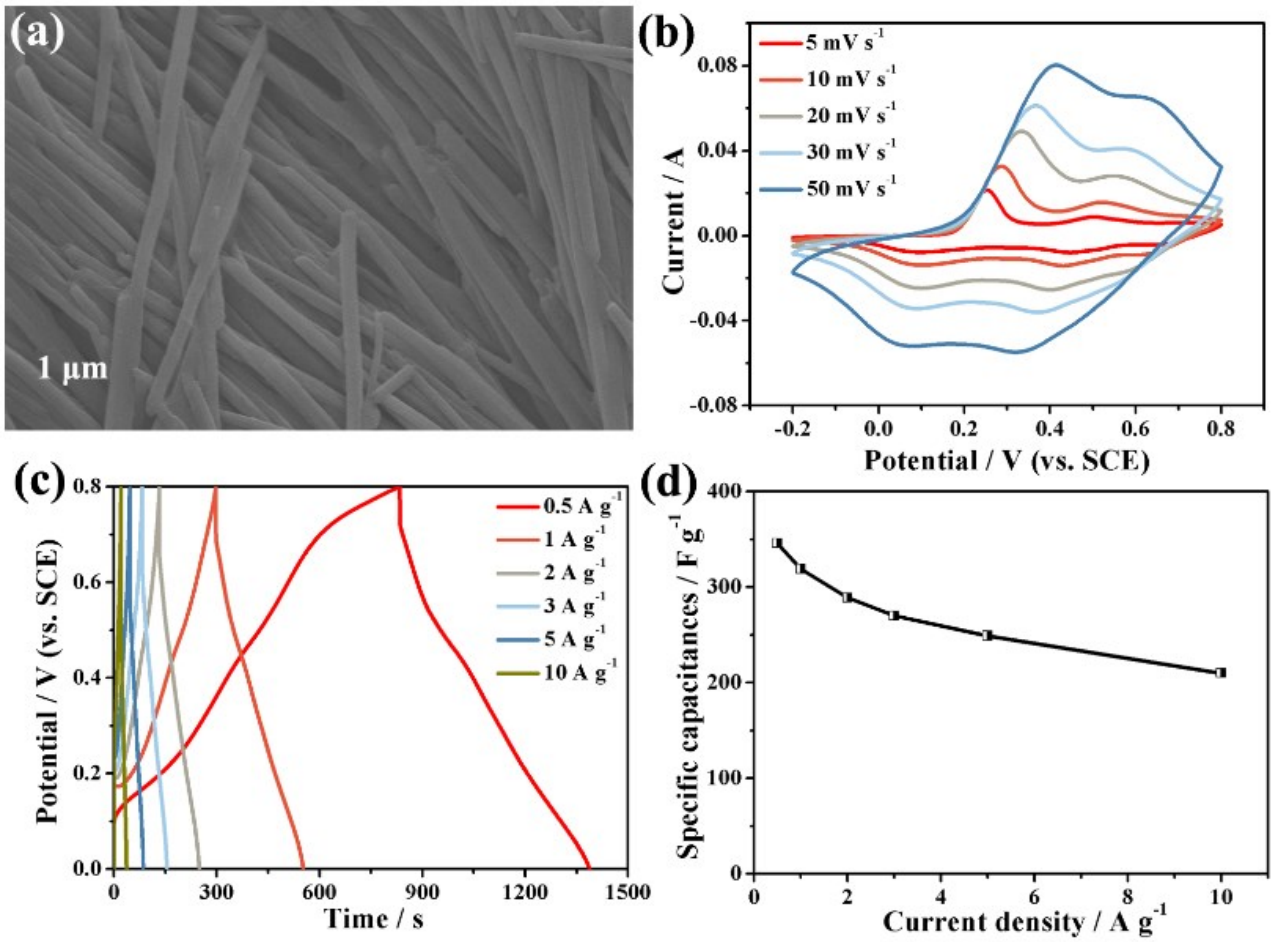

Figure S4 (a) FE-SEM image; (b) CV curves at different scan rates; (c) the GCD curves at different current densities and (d) the corresponding discharge capacitances of P(4-ADPA) without CTAB.

Depending on the scanning electron microscopy (SEM) image exhibited in Fig. S4a, the P(4-ADPA)-L-CTAB free exists in the form of adhesive nanoribbons structure, while P(4-ADPA)-L using CTAB as structure-directing agent has uniform intertwined nanosheets structure. It is clear that the existence of CTAB can provide as-prepared polymer some spaces between each ribbons and extend nanoribbons into nanosheets, offering numerous reaction sites, facilitate effective charge transport and ionic diffusion and thereby increase their capacity. Additionally, the electrochemical properties of P(4-ADPA)-L-CTAB free was shown in Fig S4b-d. As shown in Fig S4b, the shape of CV curves of P(4-ADPA)-L-CTAB free has no obvious different from its original shape with the increasing scan rate, demonstrating its fast electrochemical response and good rate capability. And GCD curves of P(4-ADPA)-L-CTAB free (in Fig. S4c) are always symmetric mirror-like feature with the increasing current density, illustrating a highly reversible redox reaction during charge/discharge process. As

depicted in Fig. S4d, P(4-ADPA)-L-CTAB free has lower capacitance (346 F g^{-1}) than that of P(4-ADPA)-L (388 F g^{-1}) at the current density of 0.5 A g^{-1}. Additionally, the capacitance retention ratio of P(4-ADPA)-L-CTAB free is 61% accompanied by the current density up to 10 A g^{-1} which is also lower than P(4-ADPA)-L.

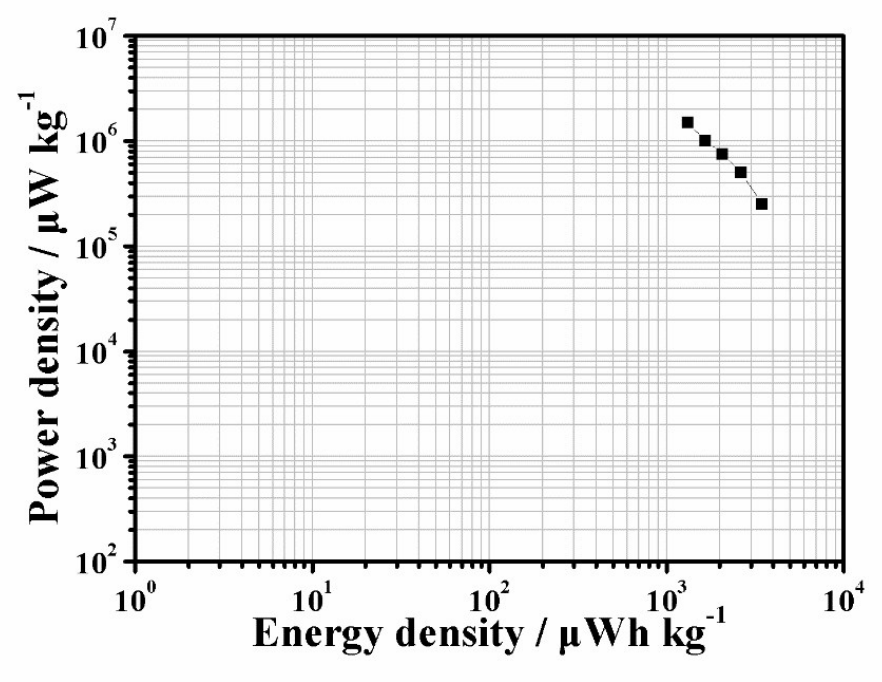

Figure S5 Ragone plot related to energy and power densities of P(4-ADPA)//P(4-ADPA).

Table S1 Performances comparison of various conductive polymer materials in the references.

Material	Discharge Rate	Operation voltage (V)	Electrolyte	Specific Capacitance ($F\ g^{-1}$)	Refs.
P(4-ADPA)-L	0.5 A g^{-1}	-0.2-0.8	1 M H_2SO_4	388	This work
Mo_2N@PANI	0.5 A g^{-1}	-0.45-0.45	1 M H_2SO_4	111.8	1
C/GF/PANI	80 mA cm^{-2}	-0.8-0.6	1 M H_2SO_4	357	2
$MnFe_2O_4$/Carbon black/ PANI	0.5 A g^{-1}	-0.2-0.6	0.5 M H_2SO_4	204.3	3
PANI/$MnFe_2O_4$	1.0 A g^{-1}	-0.2-1.0	1 M H_2SO_4	371	4
PANI/RGO-SiO_2	0.2 A g^{-1}	0-0.8	1 M H_2SO_4	360	5
PANI particles	0.5 A g^{-1}	0-0.7	1 M H_2SO_4	352	6
PANI layered flowers	1.0 A g^{-1}	0-0.8	1 M H_2SO_4	272	7
PANI/CNT	0.5 A g^{-1}	-0.2-0.6	1 M H_2SO_4	385	8
PANI-CNF	1.0 A g^{-1}	-0.4-0.6	1 M H_2SO_4	234	9

Table S2 The value of equivalent series resistance and Warburg resistance of all the P(4-ADPA).

Material	Equivalent series resistance (Ω)	Warburg resistance (Ω)
P(4-ADPA)-H	1.87	0.44
P(4-ADPA)-S	1.31	0.38
P(4-ADPA)-P	1.45	0.35
P(4-ADPA)-M	1.71	0.36
P(4-ADPA)-C	1.65	0.42
P(4-ADPA)-L0.5	1.23	0.44
P(4-ADPA)-L2	1.07	0.42
P(4-ADPA)-L	0.95	0.01

References

[1] T. He, W. Zhang, P. Manasa, F. Ran, Quantum dots of molybdenum nitride embedded in continuously distributed polyaniline as novel electrode material for supercapacitor. Journal of Alloys and Compounds 812 (2020) 152138.

[2] K. Sharma, K. Pareek, R. Rohan, P. Kumar, Flexible supercapacitor based on three-dimensional cellulose/graphite/polyaniline composite. International Journal of Energy Research 43 (2019) 604-611.

[3] D. Zha, P. Xiong, X. Wang, Strongly coupled manganese ferrite/carbon black/polyaniline hybrid for low-cost supercapacitors with high rate capability. Electrochim. Acta 185 (2015) 218-228.

[4] N. Arsalani, A.G. Tabrizi, L.S. Ghadimi, Novel PANI/$MnFe_2O_4$ nanocomposite for low-cost supercapacitors with high rate capability. J. Mater. Sci. Mater. Electron. 29 (2018) 6077-6085.

[5] J. Kim, M. Kim, S.H. Cho, C.M. Yoon, C. Lee, J. Ryu, J. Jang, Multidimensional polyaniline/reduced graphene oxide/silica nanocomposite for efficient supercapacitor electrodes. ChemNanoMat 2 (2016) 236-241.

[6] Y. Gawli, A. Banerjee, D. Dhakras, M. Deo, D. Bulani, P. Wadgaonkar, M. Shelke, S. Ogale, 3D polyaniline architecture by concurrent inorganic and organic acid doping for superior and robust high rate supercapacitor performance. Sci. Rep. 6 (2016) 21002.

[7] Y. Ma, C. Hou, H. Zhang, M. Qiao, Y. Chen, H. Zhang, Q. Zhang, Z. Guo, Morphology-dependent electrochemical supercapacitors in multidimensional polyaniline nanostructures. J. Mater. Chem. A 5 (2017) 14041-14052.

[8] S. K. Simotwo, C. DelRe and V. Kalra, Supercapacitor electrodes based on high-purity electrospun polyaniline and polyaniline−carbon nanotube nanofibers. ACS Appl. Mater. Interfaces 8 (2016) 21261-21269.

[9] M. Yanilmaz, M. Dirican, A. M. Asiri, X. Zhang, Flexible polyaniline-carbon nanofiber supercapacitor electrodes. Journal of Energy Storage 24 (2019) 100766.